Lab on a Chip

Accepted Manuscript

ROYAL SOCIETY OF CHEMISTRY

www.rsc.org/loc

Design and fabrication of magnetically functionalized flexible micropillar arrays for rapid and controllable microfluidic mixing

Bingpu Zhou,[a,†] Wei Xu,[b,†] Ahad A Syed,[b] Yeungyeung Chau,[a] Longqing Chen,[b] Basil Chew,[b] Omar Yassine,[c] Xiaoxiao Wu,[d] Yibo Gao,[a] Jingxian Zhang,[e] Xiao Xiao,[d] Jürgen Kosel,[c] Xi-Xiang Zhang,[b*] Zhaohui Yao,[e] and Weijia Wen[a,d,*]

[a]Nano Science and Technology Program and KAUST-HKUST Micro/Nanofluidic Joint Laboratory, The Hong Kong University of Science and Technology, Clear Water Bay, Kowloon, Hong Kong

[b]Advanced Nanofabrication, Imaging and Characterization Core Lab, King Abdullah University of Science and Technology, Thuwal 23955-6900, Kingdom of Saudi Arabia

[c]Computer, Electrical and Mathematical Sciences and Engineering Division, King Abdullah University of Science and Technology, Thuwal 23955-6900, Kingdom of Saudi Arabia

[d]Department of Physics, The Hong Kong University of Science and Technology, Clear Water Bay, Kowloon, Hong Kong

[e]Department of Engineering Mechanics, Tsinghua University, Beijing, P. R. China

[*]Authors to whom correspondence should be addressed; E-mail: xixiang.zhang@kaust.edu.sa, phwen@ust.hk; Fax: +852 23581652; Tel: +852 23587979

[†]Bingpu Zhou and Wei Xu are co-first authors and contributed equally to the work.

Abstract

Magnetically functionalized PDMS-based micropillar arrays have been successfully designed, fabricated and implanted for controllable microfluidic mixing. The arrangement of PDMS micropillar arrays inside the microchannel can be flexibly controlled by external magnetic field. As a consequence, the flow fields inside the microchannel can be regulated at will via magnetic activation conveniently. When a microchannel implanted with such micropillar arrays, two microstreams can be mixed easily and controllably upon the simple application of an on/off magnetic signal. Mixing efficiencies based on micropillar arrays with different densities were

investigated and compared. It was found that micropillar arrays with higher density (i.e. smaller pillar pitch) would render better mixing performance. Our microfluidic system is capable of generating highly reproducible results within many cycles of mixing/non-mixing conversion. We believe that the simple mixing-triggering method together with rapid and controllable mixing control will be extraordinarily valuable for various biological or chemical applications in the future.

Introduction

Rapid and homogenous mixing of two or more liquids is of great importance in microfluidic systems for various chemical and biological processes [1-4]. Mixing is however generally challenging in miniature devices due to the intrinsic laminar characteristics [5, 6]. During the past years, a variety of passive and active micromixers have been developed to improve the mixing efficiency. Passive mixers rely mainly on molecular diffusion or chaotic advection inside the microchannel [7-10]. Such mixing process does not require external stimulus but relies on the geometric design to passively stretch or disrupt the fluid interfaces for enhanced mass transfer. Despite the low cost or no required stimulus, passive mixers generally demand a prohibitively long mixing route (a few centimeters) and lack the flexibilities of controllable mixing due to the pre-defined flow fields [11].

In contrast, active mixers introduce external energy to generate perturbation for mixing effectuation [12]. To date, various triggering approaches, e.g. pressure [13], acoustic [14], and electric [15], have been extensively developed for microfluidic applications. Normally, active mixers can yield better mixing results and are more controllable [16, 17]. However, most active mixers demand high power to achieve optimal results which usually lead to undesirable effects on targets such as cell or DNA. Furthermore, the integration of on-chip transducers (e.g. electrodes or valves) generally complicates the whole system and limits the compatibility with other on-chip components [18]. As a consequence, it is necessary to search for advanced approaches aiming at fast and controllable mixing while not complicating the whole microfluidic system.

In recent years, magnetism has been proved to be a promising fluid manipulation means in various microfluidic applications, such as sorting [19, 20], pumping [21, 22], trapping [23, 24], and propulsion [25]. Magnetism-based fluid manipulation has advantages over other active types, including contactless communication between stimulus and targets, immunity from pH values or

surface charges, and its non-invasive nature [26, 27]. Magnetism-based approach has already been well utilized for mixing control in microfluidic systems, such as mixing in parylene microchip by integrated magnetic stir bar under a rotating magnetic field [28, 29]. Ferrofluid was also reported as an efficient mixing medium inside the microfluidic chamber where full mixing could be obtained with a low magnetic flux density [30].

Recently, artificial micropillars with embedded magnetic particles were successfully applied for mixing control under diverse magnetically actuated beating motions [31, 32]. For example, Chen et al. integrated a single magnetic micropillar array inside the microchannel for mixing enhancement. In their work, a built-in magnetic coil system was adopted to induce various beating trajectories of the artificial cilia which finally helped to actuate mixing. Even though enhanced mixing could be obviously observed in such magnetism-based approaches, external coil drivers are commonly required in order to generate dynamic magnetic field for cilia motion control. Such requirement of peripheral hardware may lead to a burdensome microfluidic system which would hamper the scope of wide employment for some particular aspects.

Considering the superior properties of magnetism-based approach while avoiding the consequent drawbacks, here we demonstrate that with the convenient application of an on/off external magnetic signal, microfluidic mixing can be rapidly and controllably achieved within milliseconds. With embedded magnetically functionalized micropillars, the fluid field inside the microchannel can be flexibly regulated based on the on/off static magnetic stimulus. In this work, the dimensional parameters of the micropillars have been greatly reduced to 5 μm in diameter and 55 μm in height, which enhances the integration capability of such magnetism-based micromixer to the microfluidic chip. Unlike most magnetism-based micromixers, the presented method requires no sophisticated beating drivers to precisely control the motion of the micropillars for mixing activation, which provides researchers a facile mode for on-chip rapid and controllable bio/chemical assays.

Experimental Procedure

Design Principle

The overall 3D architecture of the micromixer is presented in Fig. 1a. The microfluidic device contains

two liquid inlets (A and B), one shared outlet, and a straight microchannel with integrated magnetically functionalized polydimethylsiloxane (PDMS) micropillar arrays. The covering length of micropillars along the x direction is about 6 mm. The diameter (D) of each micropillar was set to be 5 μm while for pitches (P) between two adjacent pillars, we have designed three kinds of micromixers, namely of 15 μm, 25 μm and 35 μm.

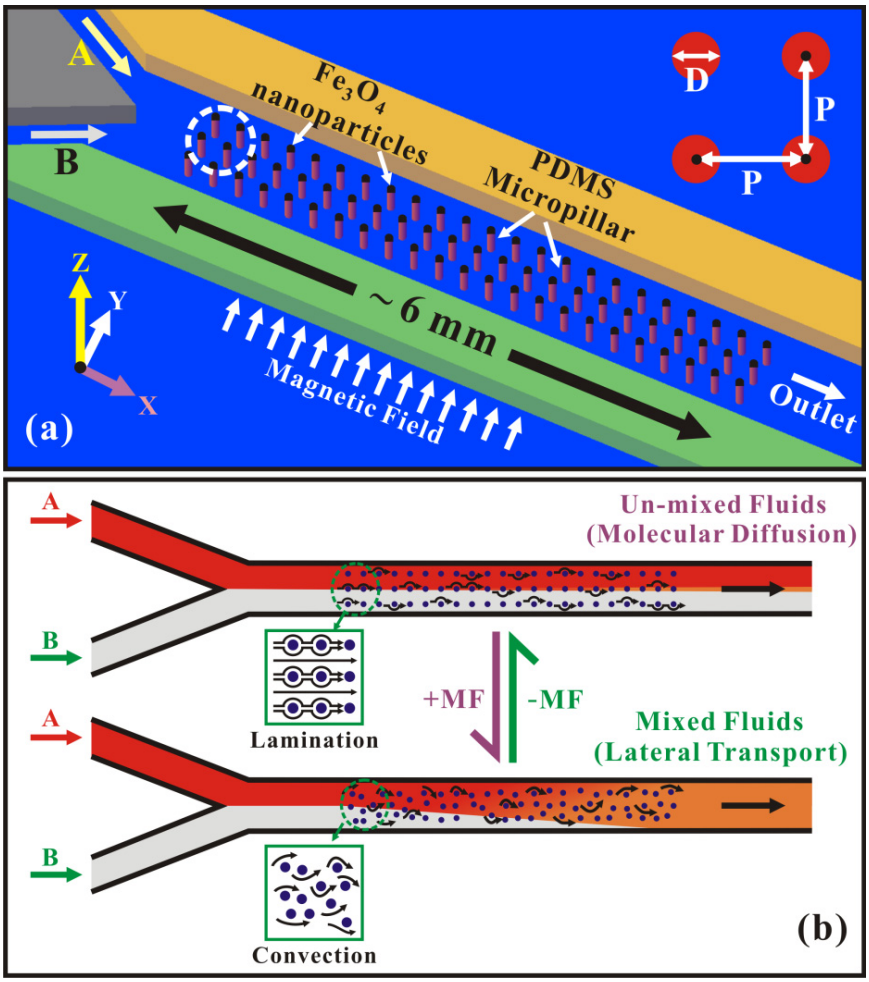

Fig. 1(a) 3D Schematic of the micromixer based on embedded magnetically functionalized PDMS micropillars; (b) Working principle of the micromixer by magnetic actuation.

Fig. 1b shows how the embedded magnetically functionalized PDMS micropillars that can be introduced as a useful medium for rapid and controllable mixing regulation. Without application of magnetic field (NO MF), the micropillars maintain their initial shape and stand vertically inside the microchannel in a uniform format. Unlike other passive mixers which rely on embedded artificial obstacles [33, 34], the micropillars here have scant impact on distorting the flow field due to the

relatively small size when compared to the channel width (200 μm). As a consequence, fluids pass by the symmetrically arranged micropillars without obviously enhanced mixing and the mixing efficiency is dominated by diffusion. However, when magnetic field is applied (MF ON), the magnetic force reorients the free ends of the PDMS micropillars owing to the elastic characteristic. The orientation of the applied MF was along the y direction of the microchannel. Thanks to the small gaps between the elastic micropillars, they tend to touch the neighboring ones during the bending process and produce a random and disorganized configuration inside the microchannel (as given by the blue dots). The induced disorder and asymmetry lead to different resistance to the incoming flow along the microfluidic channel such that fluids tend to find the path with lower hydrodynamic resistance [33]. The consequence is that fluid flow was distorted and lateral mass transport can be extensively enhanced when fluids pass by the micropillar region. Thus, the mixing efficiency will be raised upon MF triggering. While retracting the MF, the pillars return to their original vertical and ordered position and fluids pass by with molecular diffusion only.

Through this means, the mixing/non-mixing convertibility can be simply regulated by applying a static on/off external magnetic field at will without complicating the whole system. In this experiment, the MF is provided by an NdFeB permanent magnet (diameter of ~ 2 cm, magnetic flux density of about 200 mT at a distance of 2 mm from the surface). Mixing would be actuated by simply placing a magnet closely under the microfluidic chip and ceased by removing the magnet from the microfluidic system.

Fabrication of microchip with embedded magnetically functionalized PDMS micropillars

The magnetically functionalized PDMS micropillar arrays, integrated inside the microfluidic channel, were fabricated through a casting replica process (Fig. 2). The process included four main steps as follows:

i) Silicon mold processing.

The mold of microfluidic channel with integrated array of 5 μm microholes was fabricated by standard UV photolithography and DRIE dry-etching on a clean silicon wafer. The depth of the microchannel was defined as ~60 μm while the depth of the holes was ~55 μm by precisely adjusting the dry-etching process. After that, the silicon mold was silanized with

(tridecafluoro-1,1,2,2-tetrahydrooctyl)-1-trichlorosilane for 4 days in a sealed vacuum chamber.

ii) Magnetic nanoparticle filling.

Fe_3O_4 nanoparticles were suspended in acetone solution with a concentration of ~30% (weight: volume × 100%). To promote the dispersion of nanoparticles, the suspension was agitated in the ultrasonic bath (2510 E-DTH, Branson) for 3 hours before use. After that, a drop of 1mL of the suspension was loaded onto the patterned region. A strong permanent magnet (size of 1 × 1 inch) was simultaneously attached closely to the back side of the silicon mold and kept swirling for 2mins around the patterned region to assist filling of nanoparticles into microholes. Then, the magnet was quickly removed with unfilled nanoparticles from the patterned region. The unfilled nanoparticles were then carefully scrapped from the mold by Kimwipes paper.

iii) Fabrication of PDMS micropillars.

PDMS base mixed with curing agent at 10:1 ratio was poured over the patterned region of the mold and placed in the vacuum oven for de-gas, to force the air trapped inside the microholes out so that PDMS gel could completely fill in the microholes. The PDMS and the mold were then placed on the hotplate to cure at 100 °C for 8 minutes. After curing, the PDMS layer was gently peeled off in ethanol solution and kept inside the ethanol for ease of releasing and sustaining micropillars at the same time.

Finally, the PDMS chip was dried in a CO_2 supercritical point dryer machine (Automegamdri-916B series C, Tousimis) to prevent the micropillars from collapsing during the drying process induced by the capillary force.

iv) Microchannel sealing.

Plasma bonding (Harrick Plasma, PDC-002) was introduced to seal the microfluidic channel. During the plasma bonding process, the micropillar region was covered by a small piece of PDMS in order to prevent damage to the microstructure. After 2 mins of plasma bonding, the microchannel was tightly bonded to another flat PDMS slab. A 10 mins soft-baking process (100 °C) concluded the total fabrication process.

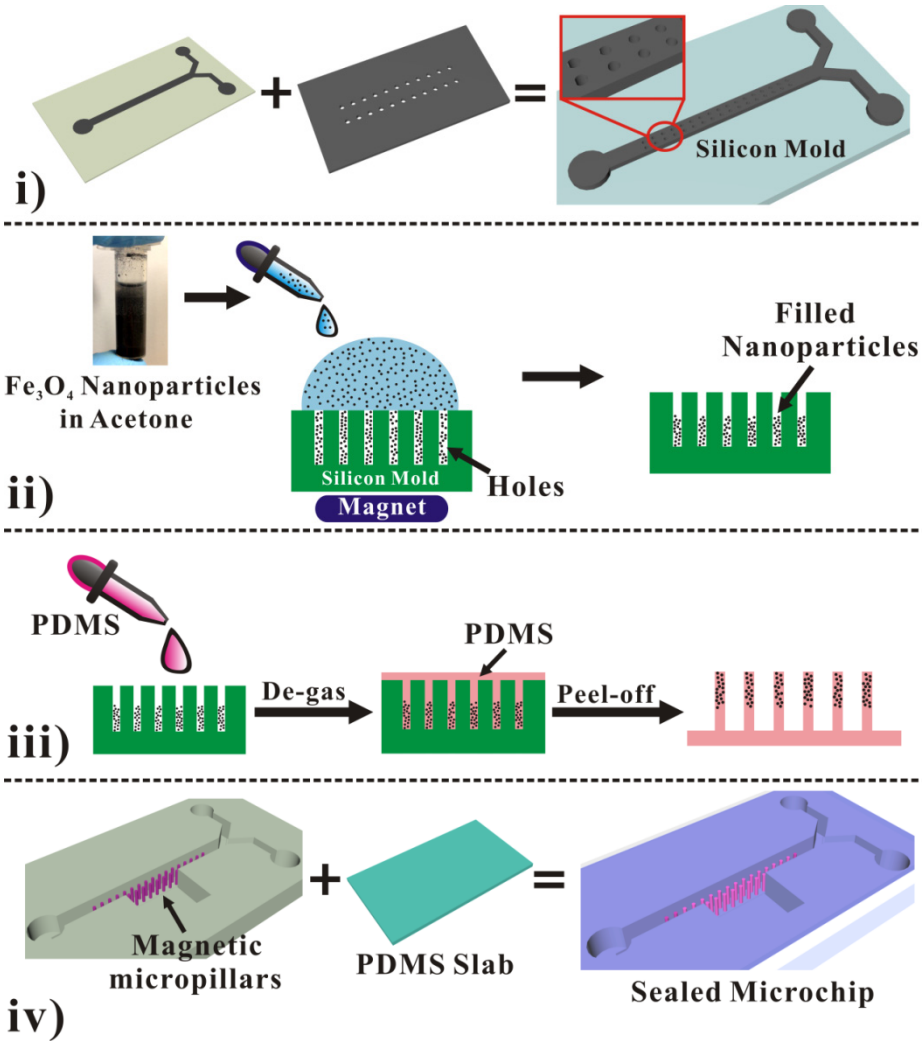

Fig. 2 Fabrication process of microchip with embedded magnetically functionalized PDMS micropillar arrays.

Characterization of microchip with embedded magnetically functionalized PDMS micropillars

Fig. 3a shows the optical image of the micromixer which has a size comparable to that of a one Hong Kong dollar coin. Red-dyed sunflower oil has been poured into the microchannel for a better contrast. Inset SEM image gives the top-view of the PDMS micropillars with diameter of 5 μm and pitch of 15 μm (green rectangle). As shown in Fig. 3b, although the micropillars exhibit vertical and ordered arrangement with no MF, they tend to incline and attach to the adjacent ones with applied MF. It could also be clearly observed that for the micropillars with pitch of 15 μm, almost all tilted pillars attached with the adjacent ones which formed a highly disordered network inside the microchannel when compared to the other two cases. Furthermore, after removing the magnetic field, micropillars can easily recover to their initial positions as mentioned. By this means, the shape of micropillars can be tuned with application of an on/off magnetic signal for all three micromixer types.

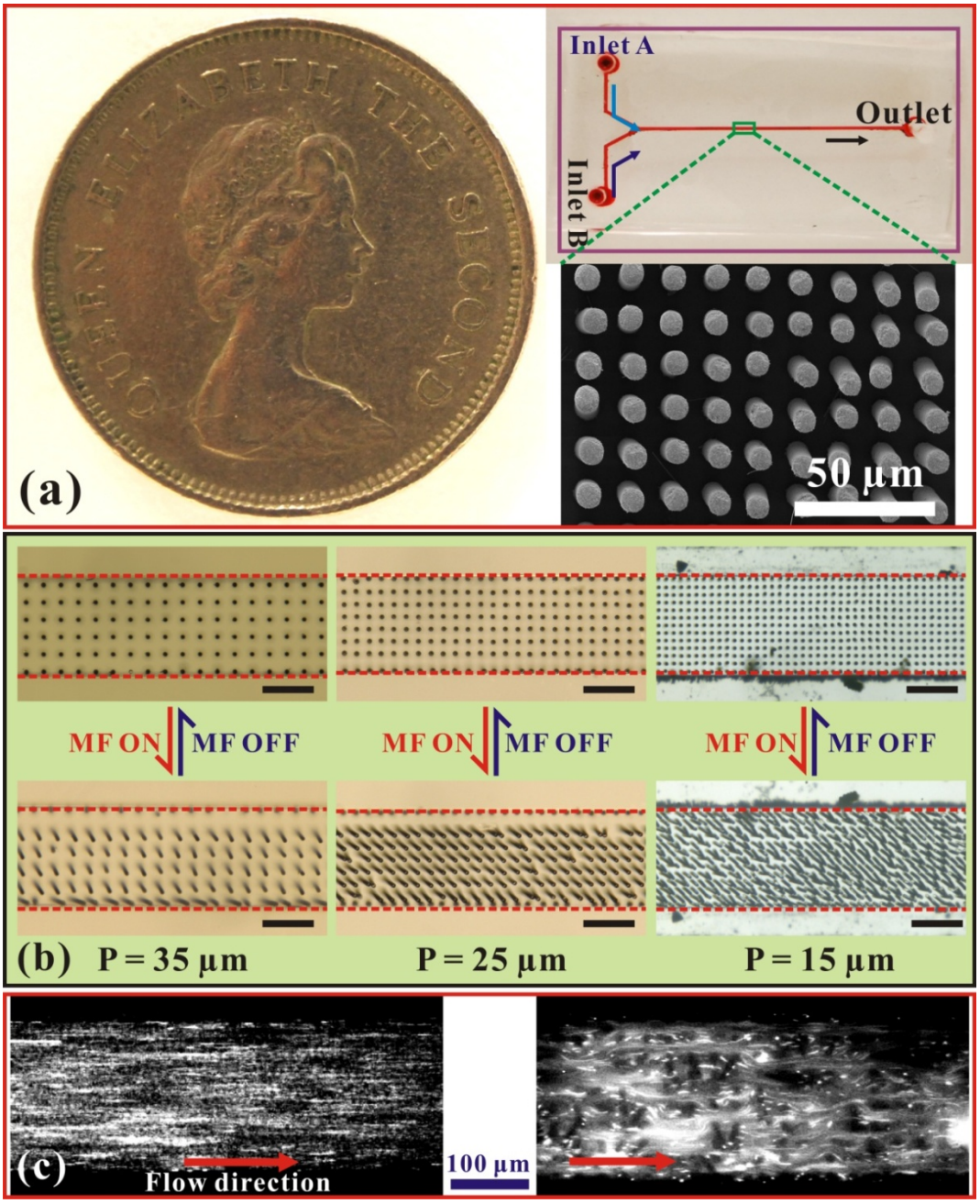

Fig. 3 (a) Optical image of the micromixer which shows a comparable size to a HongKong dollar coin; (b) Transformation of micropillar arrangements under the control of the magnetic field, scale bar: 100 μm; (c) Characterization of flow patterns without pillars and with disordered pillars inside the microchannel.

We also compared the flow pattern inside the microchannel at the location without pillars with the one with disordered pillars when MF was applied onto the microfluidic system. For this purpose, deionized water (DI-water) containing 530 nm Nile Red fluorescent particles (Spherotech Inc., USA) was continuously perfused into the microchannel with a constant flow rate of 0.05 ml/h. The left part of Fig.

3c shows the flow pattern of fluorescent nanoparticles inside the microchannel without micropillars. The figure clearly shows that the nanoparticles all followed the flow field which exhibited an almost completely laminar characteristic. When passing by the random arranged pillar arrays, the nanoparticles interacted with disordered pillars leading to a multi-directional motion of the particles in the microchannel (the right image of Fig. 3c). This phenomenon also convinced us that disordered micropillar arrangements could markedly distort the flow field and enhance the lateral redirected fluid activity.

Mixing efficiencies under different flow rates

To systematically demonstrate the mixing performance of the presented micromixer controlled by the MF, we injected DI water and fluorescent dye (fluorescein $C_{20}H_{12}O_5$, Sigma-Aldrich Co., USA) simultaneously by an external syringe pump (PHD2000, Harvard Apparatus, Holliston, USA) at the same flow rate. The fluorescent images at positions A and B (red circles in Fig. 4a) were captured in real-time under the fluorescence microscopy (IX71, Olympus Corporation, Tokyo, Japan). Corresponding gray-scale fluorescent intensity profiles across the microchannel were then figured out by ImageJ (Version 1.47, National Institutes of Health, USA). Fig. 4b shows the fluorescent image of position A and the corresponding intensity profile which represents an obvious concentration distinction between the two injecting streams. During the experiment, we gradually increased the flow rates to observe the mixing efficiency under different flow conditions. The right part of Fig. 4 gives the fluorescent images and intensity profiles at position B of the three micromixer types under flow rates of 0.10 ml/h, 1.0 ml/h, 3.0 ml/h and 5.0 ml/h. Here B1s are the images taken when no MF was applied and B2s stand for the situation when MF was imposed. With the application of external magnetic field, we can apparently discover enhanced mixing effects (B2) when compared to the images without MF (B1) for each flow condition as revealed in the intensity profiles. For fluorescent images and intensity profiles under other investigated flow rates, please refer to the supplementary material for more information (Figure S1).

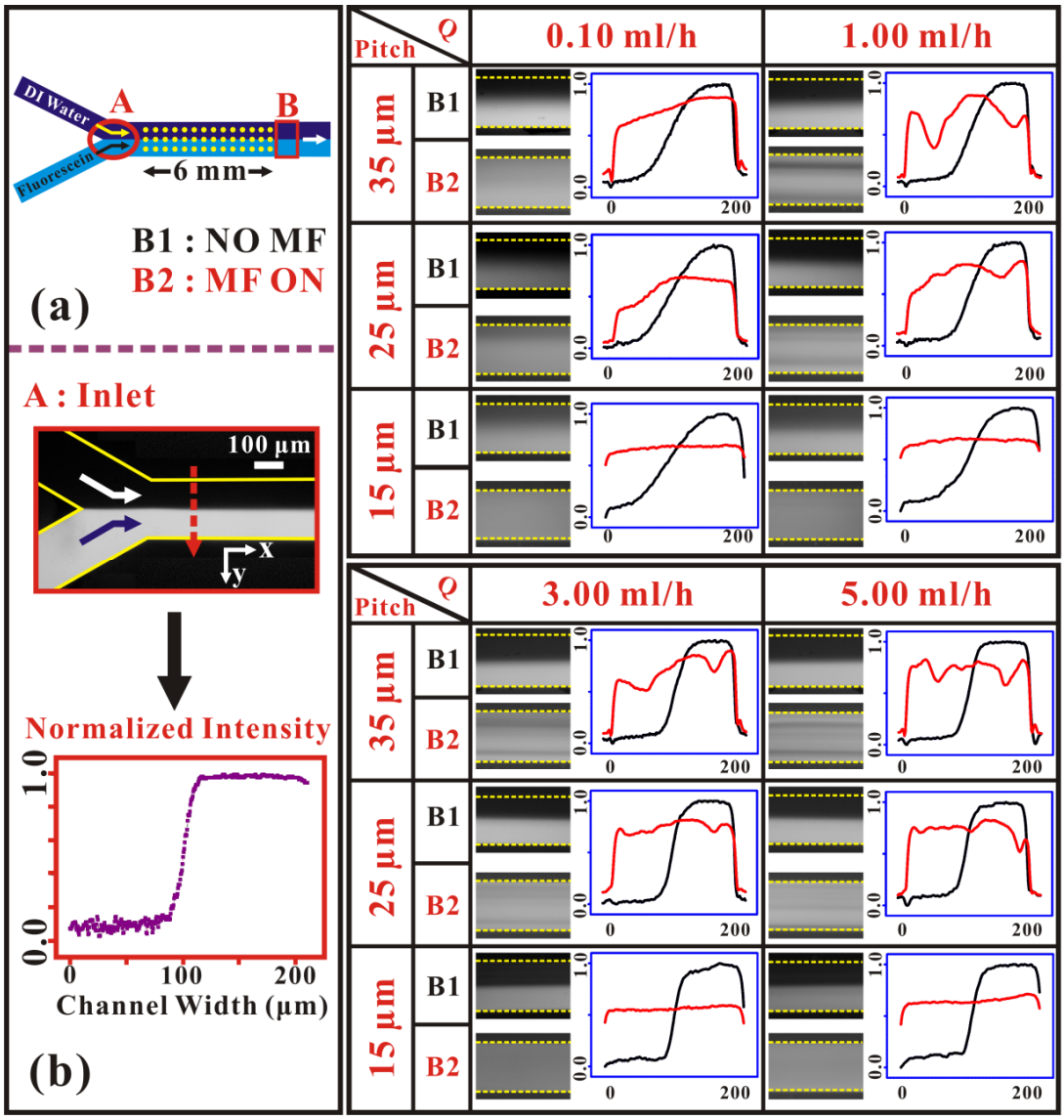

Fig. 4 (a) Schematic of the microfluidic system to be analyzed for fluorescent intensity profiles; (b) Images of fluorescent intensity profiles along the cross-section at the inlet location (referred to Fig. 4a); the corresponding normalized intensity was also provided which shows an obvious intensity difference between the two injecting streams. The right part shows the fluorescence microscopy images at location B under different flow rates ranging from 0.10 ml/h to 5.0 ml/h.

In order to statistically quantify the mixing degree, mixing index (MI) was introduced from the normalized intensity distributions along the transverse cross-section of the microchannel as below [17, 28]

$$MI = \sqrt{\frac{1}{N}\sum_{i=1}^{N}\left(\frac{c_i - \overline{c}}{\overline{c}}\right)^2} \qquad (1)$$

where N is the total sampling number, c_i the specific concentration at a considered point along the microchannel width, and $\bar{c}$ the average of c_i over N samples. When MI = 1 it is a non-mixing situation, and when MI = 0 it gives an ideal mixing outcome of the two interested solutions. Fig. 5 shows the mixing indices of three micromixer types with and without MF. From the figure, we can easily find out the trends of the mixing performance as follows:

i) In absence of the magnetic field (NO MF), the magnetically functionalized micropillars normally maintained vertical and aligned shapes inside the microchannel. The incoming fluids preserved the laminar streamlines while passing through the pillars. In this case, molecular diffusion is dominant which determines the final mixing performance. As a consequence, lower flow rates will ensure longer residence time and thus achieving better mixing degree (leading to a smaller MI).

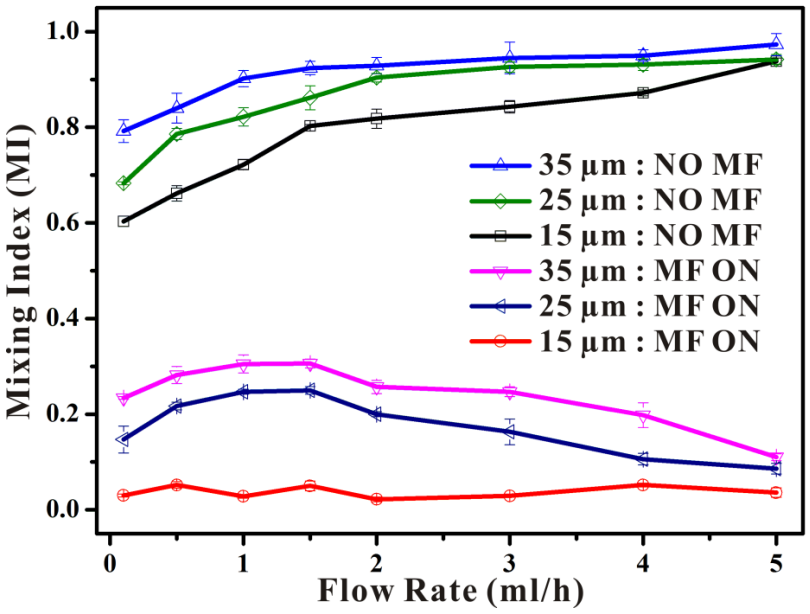

Fig. 5 Mixing indices of three micromixer types under different flow rates.

ii) When MF was applied to the microfluidic system, mixing indices of all three types of micromixers decreased dramatically compared to the ones without MF. Taking the pitch of 15 µm as an example, at flow rate of 0.5 ml/h, MI decreased from 0.662±0.016 to 0.052±0.007 when MF was applied. While for the flow rate of 5.0 ml/h, MI decreased notably from 0.938±0.007 to 0.036±0.010.

The trends of MI remained almost the same for pitches of 25 µm and 35 µm when MF was applied. At low flow rates within the range of 0.1 ml/h ~ 1.0 ml/h, both MIs increased with the increase of flow rates. While for higher flow rates above 1.0 ml/h, however, both MIs decreased with

increased flow rates. A possible explanation is that for fixed pitch between the micropillars, the Reynolds number of the microfluidic system will be mainly affected via the volumetric flow rates. At low flow rates, Reynolds number was relatively small and in this case, mixing was dominated by diffusion even though with the chaotic advection [33]. As a result, mixing efficiency gradually decreased with increased flow rates due to the reduction of residence time, for which a slight increase of MI can be found from both graphs. However, with relatively higher flow rates within range of 1.0 ml/h ~ 5.0 ml/h, higher Reynolds number will lead to the outcome that chaotic advection became dominant for mixing performance when compared with molecular diffusion. In addition, the chaotic advection slightly enhanced with increased flow rates. As a consequence, MI gradually decreased with the increase of the flow rates.

Furthermore, it was also found that almost complete mixing can be achieved within a wide range of flow rates (0.1 ml/h ~ 5 ml/h) for the smallest pitch (15μm). This is because with such a high density of micropillars, chaotic advection between two confluent streams gets more obvious and a higher disorder of the micropillars renders a better transverse mass transfer in this condition.

iii) As shown in Fig. 5, the mixing performance with various pitches of the micropillars differs from each other under a particular flow rate. In order to figure out the effect of the pitch on the mixing performance, we introduce the Reynolds number (*Re*) to investigate the relationship between the pitch and the mixing outcomes. Here we would discuss about the *Re* of the micropillars which play an important role in defining the mixing index. The Reynolds number of the micropillars is given by

$$Re_{pillar} = \frac{l \cdot \upsilon}{\nu} \qquad (2)$$

where l is the characteristic diameter of the investigated pillars, υ is the average velocity, and ν is the kinetic viscosity. As l and ν are constants in our microfluidic system for all three types of micromixers, *Re* of the micropillars will be mainly affected by the involved velocity. With a relatively smaller pitch, more micropillars can be placed across the cross-section of the microfluidic channel. This means that the localized velocity of the fluid flow will increase due to the more compact design of obstacles inside the microchannel. Consequently, the Reynolds number will relatively increase with the decrease of the pitch for a given flow rate. By this means, the mixing performance will be correspondingly better with a smaller pitch between pillars due to the higher values of *Re*. In addition, for the case of smaller pitch, more arranged micropillars inside the fluid channel will favor a higher degree of lateral

fluid transfer, which also provide inevitable benefits for enhancing the mixing performance. From this perspective, we can conclude that a denser pillar arrangement (smaller pitch between micropillars) inside the microchannel can help to generate more enhancements to the mixing efficiency.

Rapid and controllable mixing

To precisely characterize the controllable mixing performance, a computer-regulated manipulator was adopted to control the magnet for triggering mixing without manual operation (Fig. 6a). It should be noted that the introduction of the manipulator here was only intended to reduce manual error while investigating the mixing performance of our micromixing strategy precisely. A permanent NdFeB magnet with diameter of 2 cm was horizontally placed on a steel plate whose position can be precisely defined by the preset command. Here, the period of the application and retraction of the magnet is 1.0 s and the pumping flow rate was set to be 0.50 ml/h. In this way, the manipulator functioned as a switch which can turn the MF on or off periodically as defined. For the demonstration, blue ink dye solution and deionized-water were simultaneously injected into the microfluid channel with the same flow rate. Fig. 6b gives typical time-lapse images of the controllable mixing behaviors triggered by magnetic signal. Initially, when magnetic field was absent (t = 0 s), obvious interface between two microstreams was observed. With application of the magnetic field, it could be clearly found that mixing was quickly enhanced within milliseconds. After we withdrew the magnetic field (t = 0.5 s), the two microstreams returned to the original state without enhanced mixing. Furthermore, with the existence of magnetic field (t = 1.0 s), mixing was actuated again as shown in the series of the images (from t = 1.0 s to t = 1.5 s).

Fig. 6c shows the dispersion of the blue ink dye along the cross-section of the microchannel under successive application and removals of MF from the microfluidic system. Clear interface between two streams can be found without MF while evident mixing could be achieved once MF was applied to the system. The series of photos demonstrated that the mixing/non-mixing performance could be quickly switched in a highly reproducible manner. From the result, we can also confirm that the magnetically functionalized pillars can swiftly respond in the microchannel to the external magnetic stimuli in milliseconds. Real-time recording video of such mixing process can be found in the supplementary electronic material.

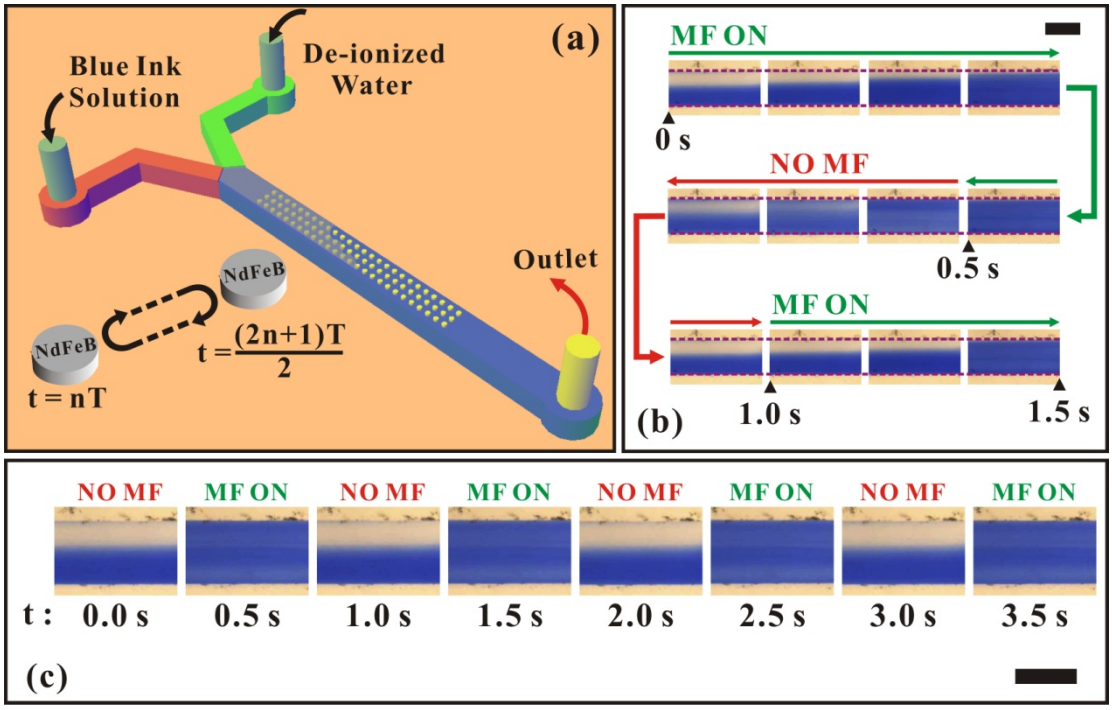

Fig. 6 (a) Schematic for controllable mixing. The position of the permanent magnet was precisely controlled by a computer-regulated manipulator. (b) Time-lapse recordings of mixing performance. MF ON means application of magnetic field while NO MF means removal of magnetic field from the microfluidic system; (c) Dispersion of blue ink dye inside the microchannel with application (MF ON) and removal (NO MF) of magnetic field. All scale bars in the figures are 200 μm.

Conclusion

In this work, we successfully demonstrated the capacity of rapid and controllable mixing by introducing magnetically functionalized PDMS micropillars without any sophisticated beating equipment. With response to simple application/retraction of magnetic stimulus, the embedded PDMS micropillars were successfully introduced to regulate fluid flow and thus control the final mixing degrees.

The mixing performances of three micromixer types, namely pitches of 15 μm, 25 μm and 35 μm, were comprehensively investigated within flow rates from 0.10 ml/h to 5.0 ml/h. It was shown that smaller pitch can induce better mixing efficiency with application of a magnetic field. In addition, for the smallest pitch of 15 μm, almost complete mixing was well observed for the covering flow rates studied.

Finally, a computer-regulated manipulator was introduced for applying to or removing the magnetic field from the microfluidic system by precisely controlling the position of the permanent magnet. The purpose of replacing manual operation was to accurately study the response time as well as the reproducibility of our proposed micromixer design. It was found that the magnetically functionalized pillars could response swiftly to the external MF stimulus within milliseconds and reverted to the initial status once the magnetic field was retracted.

To trigger microfluidic mixing without any elaborate implements, our approach provides an easy-handling and controllable scheme implied with a portable magnet. Moreover, the way of manual operation renders a more straightforward and feasible microfluidic system for real world applications. The methodology described here is particularly beneficial as superior mixing efficiency can be achieved for wide flow rate ranges with highly repeatable performance. We believe that this convenient MF-based mixing avenue can be well applicable to diverse on-chip biological or chemical assays.

Acknowledgements

This publication is based on work partially supported by Award No. SA-C0040/UK-C0016, made by King Abdullah University of Science and Technology (KAUST), Hong Kong RGC grants HKUST 604710 and 605411. The work is also partially supported by the Nanoscience and Nanotechnology Program at HKUST.

References

1. Y. Lin, G. J. Gerfen, D. L. Rousseau, and S. R. Yeh, *Anal. Chem.*, **2003**, 75, 5381.

2. R. A. Vijayendran, K. M. Motsegood, D. J. Beebe, and D. E. Leckband, *Langmuir*, **2003**, 19, 1824.

3. D. S. Kim, S. H. Lee, C. H. Ahn, J. Y. Lee, and T. H. Kwon, *Lab Chip*, **2006**, 6, 794.

4. H. Y. Lee, and J. Voldman, *Anal. Chem.*, **2007**, 79, 1833.

5. J. M. Ottino, and S. Wiggins, *Phil. Trans. R. Soc. Lond. A*, **2004**, 362, 923.

6. L. Capretto, W. Cheng, M. Hill, and X. L. Zhang, *Top. Curr. Chem.*, **2011**, 304, 27.

7. V. Mengeaud, J. Josserand, and H. H. Girault, *Anal. Chem.*, **2002**, 74, 4279.

8. A. D. Stroock, S. K. W. Dertinger, A. Ajdari, I. Mezic, H. A. Stone, and G. M. Whitesides, *Science*, **2002**,

295, 647.

9. S. H. Wong, M. C. L. Ward, and C. W. Wharton, *Sens. Actuators B Chem.*, **2004**, 100, 359.

10. A. P. Sudarsan, and V. M. Ugaz, *Lab Chip*, **2006**, 6, 74.

11. X. Mao, B. K. Juluri, M. I. Lapsley, Z. S. Stratton, and T. J. Huang, *Microfluid Nanofluid*, **2010**, 8, 139.

12. N. T. Nguyen, and Z. G. Wu, *J. Micromech. Microeng.*, **2005**, 15, R1.

13. B. Wang, J. L. Xu, W. Zhang, and Y. X. Li, *Sens. Actuators A Phys.*, **2011**, 169, 194.

14. D. Ahmed, X. Mao, J. Shi, B. K. Juluri, and T. J. Huang, *Lab Chip*, **2009**, 9, 2738.

15. M. H. Oddy, J. G. Santiago, and J. C. Mikkelsen, *Anal. Chem.*, **2001**, 73, 5822.

16. X. Z. Niu, L. Y. Liu, W. J. Wen, and P. Sheng, *Phys. Rev. Lett.*, **2006**, 97, 044501.

17. A. V. Marques, F. Barbaud, and D. Baigl, *J. Am. Chem. Soc.*, **2013**, 135, 3218.

18. P. H. Huang, Y. L. Xie, D. Ahmed, J. Rufo, N. Nama, Y. C. Chen, C. Y. Chan, and T. J. Huang, *Lab Chip*, **2013**, 13, 3847.

19. R. Rong, J. W. Choi, and C. H. Ahn, *J. Micromech. Microeng.*, **2006**, 16, 2783.

20. A. E. Saliba, L. Saias, E. Psychari, N. Minc, D. Simon, F. Bidard, C. Mathiot, J. Y. Pierga, V. Fraisier, J. Salamero, V. Saada, F. Farace, P. Vielh, L. Malaquin, and J. L. Viovy, *Proc. Natl. Acad. Sci. U. S. A.*, **2010**, 107, 14524.

21. A. Hatch, A. E. Kamholz, G. Holman, P. Yager, and K. F. Bohringer, *J. Microelectromech. S.*, **2001**, 10, 215.

22. Y. J. Chang, C. Y. Hu, and C. H. Lin, *Sens. Actuators B Chem.*, **2013**, 182, 584.

23. H. Lee, A. M. Purdon, and R. M. Westervelt, *Appl. Phys. Lett.*, **2004**, 85, 1063.

24. W. Liu, N. Dechev, I. G. Foulds, R. Burke, A. Parameswaran, and E. J. Park, *Lab Chip*, **2009**, 9, 2381.

25. S. N. Khaderi, C. B. Craus, J. Hussong, N. Schorr, J. Belardi, J. Westerweel, O. Prucker, J. Rühe, J. M. J. den Tooner, and P. R. Onck, *Lab Chip*, **2011**, 11, 2002.

26. N. Pamme, *Lab Chip*, **2006**, 6, 24.

27. N. T. Nguyen, *Microfluid Nanofluid*, **2012**, 12, 1.

28. L. H. Lu, K. S. Ryum and C. Liu, *J. Microelectromech. S.*, **2002**, 11, 462.

29. K. S. Ryu, K. Shaikh, E. Goluch, Z. F. Fan, and C. Liu, *Lab Chip*, **2004**, 4, 608.

30. G. P. Zhu, and N. T. Nguyen, *Lab Chip*, **2012**, 12, 4772.

31. A. R. Shields, B. L. Fiser, B. A. Evans, M. R. Falvo, S. Washburn, and R. Superfine, *Proc. Natl. Acad. Sci. U. S. A.*, **2010**, 107, 15670.

32. C. Y. Chen, C. Y. Chen, C. Y. Lin, and Y. T. Hu, *Lab Chip*, **2013**, 13, 2834.

33. H. Z. Wang, P. Iovenitti, E. Harvey, and S. Masood, *Smart Mater. Struct.*, **2002**, 11, 662.

34. A. A. S. Bhagat, E. T. K. Peterson, and I. Papautsky, *J. Micromech. Microeng.*, **2007**, 17, 1017.

We present a rapid and controllable microfluidic mixing strategy with magnetically functionalized PDMS-based micropillar arrays triggered via an on/off magnetic field stimulus.